Journal of Pharmaceutical Chemistry
http://www.vensel.org/index.php/jphchem
VENSEL

In silico development of a novel putative inhibitor of the 3C protease of Coxsackievirus B3 with a benzene sulfonamide skeleton

[1]Ajay Kumar Timiri, [2]Syed Hussain Basha, [3,] Rana Abdelabi, [3]Johan Neyts, [3]Pieter Leyssen, [1]Barij Nayan Sinha, [1,*]Venkatesan Jayaprakash

[1]Department of Pharmaceutical Sciences & Technology, Birla Institute of Technology, Mesra, Ranchi-835215, Jharkhand, India
[2]Innovative Informatica Technologies, Hyderabad-500049, Telungana, India
[3]Rega Institute for Medical Research, University of Leuven, Minderbroedersstraat, 10, 3000 Leuven, Belgium

Abstract: Availability of X-ray crystal structure of 3C protease of several enteroviruses provided an opportunity for *in silico* drug design and development approach. Presented study is aimed at designing a novel compound targeting 3C protease of Coxsackievirus (CVB3), which is reported frequently to cause myocarditis in North America and Europe. A pthalimido-sulfonamide derivative (ZINC13799063) was identified through high-throughput virtual screening (HTVS) approach from the top HITs. A small library of phalimido-sulphonamides was enumerated to find a potential LEAD. Compound **17** from the library was found to inhibit CVB3 selectively in cell based antiviral assay at a concentration of EC50=1.0±0.1 μM with a selectivity index of >140. Molecular dynamics study was performed to investigate the selective inhibition of CVB3 over CVB4.

Keywords: Coxsackie virus B3; Virtual Screening; protease inhibitors; Sulfonamide; Molecular dynamics

1. Introduction

Coxsackie virus (CV), a non-enveloped RNA virus belonging to the genus Enterovirus of family Picornaviridae[1] was isolated in the year 1947[2, 3]. The first major outbreak was reported in Johannesburg during 1952 that was followed by regular flare-ups every 3-6 years[4, 5]. Coxsackie viral infection in human being has been associated with myocarditis, myopericarditis, aseptic meningitis and chronic autoimmune diseases such as insulin-dependent diabetes mellitus (IDDM)[6-8]. A chronic form of the infection in females may lead to new born babies with neonatal myocarditis and/or hepatitis[9, 10]. Currently, there is no specific antiviral therapy available for the treatment of infections with this virus[5]. Although many molecules with *in vitro* antiviral activity have been reported in the literature, none has made it to the market. Worth mentioning a few: 1,2-fluoro-4-(2-methyl-8-(3-(methylsulfonyl)-benzylamino) imidazo [1,2-a]pyrazin-3-yl)phenol[11], pyrrolidine dithio-carbamate[12], 5-substituted cytidine analogues[13]. Many molecules from plants origin were also reported to have inhibitory activity on CV, few to mention: (i) benzophenone C-glucosides and gallotannins from mango tree stem bark[14], macromolecules isolated from *Phellinus pini* fruiting body[15], roots of *Phyllanthus emblica*[16], and monomers from Chinese medicinal herb *Folium isatidis*[17].

Enteroviral 3C protease belongs to trypsin-like cysteine proteases[18]. The active site of the proteases was having catalytic triad composed of His40, Glu71 and Cys147 and is conserved across picornaviruses. It is an essential multifunctional enzyme that processes nine intermediate processing events of viral cell cycle in all picornaviruses[19]. In addition, it also shuts off host cell RNA transcription[20], and targets several host proteins such as translation initiation factor G, and cleavage stimulation factor 64 to stop host protein synthesis and induce apoptosis[21-23]. As proteases of enteroviruses are having little sequence similarity with host cell proteases[24], designing molecule to hit them has been a rational approach in developing antivirals against them.

As X-ray crystal structure of 3C protease of CVB3 (PDB: 3ZZA) is available, a high-throughput virtual screening (HTVS) approach has been adopted to identify new hit compounds for drug development project. The approach (HTVS) has been successful in many cases and the readers are suggested to refer the review by Badrinarayan *et al*[25]. Our attempt has resulted some novel scaffolds as HITs at the top. One of the top-ranking compounds, ZINC13799063, a pthalimido-sulfonamide derivative captured our attention, as it was the one that was spotted in our earlier attempt with DENV protease. A library of compounds was enumerated during our earlier attempt that is structurally close to ZINC13799063 and was tested for their inhibitory activity on DENV protease[26]. We utilized the same chemical library for the current exploration of antiviral activity against CV. *In silico* methodologies were employed to obtain a deeper insight into the possible interaction at molecular level between the most potent compound **17** and the 3C protease of CVB3 and CVB4. Since the related library was in hand, we thought of screening them.

Submitted on: Jul 29, 2017 | Accepted on: Aug 06, 2017
*corresponding author: VJ Tel: +919470137264; E-mail: drvenkatesanj@gmail.com

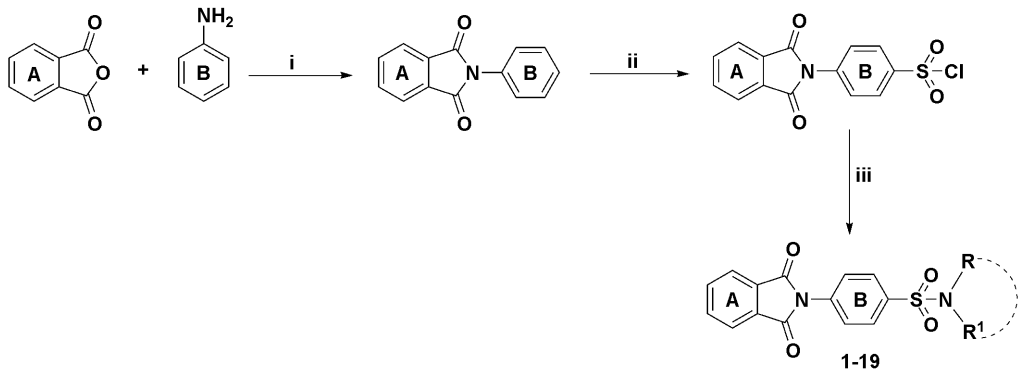

Scheme 1. Reagents and conditions: (i) AcOH glacial, reflux, 4h; (ii) PCl5, HSO3Cl, DCM, 0º C, reflux, 0.5 h; (ii) R,R1-NH, pyridine, DCM, 0º-rt C, 0.5-5 h.

The rational behind its selection was based on the fact that sulfonamides has the ability to mimic the peptide bond and increases the resistance towards protease-catalyzed degradation[27]. Furthermore, sulfonamides have previously been successfully incorporated in many peptidomimetics[28, 29] and have also been reported as protease inhibitors of HIV[30] and HCV[31].

2. Result and Discussion

2.1 Synthesis

A small library of nineteen compounds was designed and synthesized based on the structure of one of the top hit (ZINC13799063) from the HTVS study. The designed compounds were having benzene ring in place of pyridine, a bioisosteric replacement (Figure 1). Synthesis of the compounds was achieved by following the reactions outlined in Scheme 1. For the synthetic procedure and characterization data of the library compounds, readers are suggested to refer our earlier publication.[26]

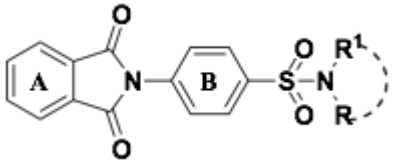

Figure 1. General structure of compounds **1-19**

2.2 Antiviral activity

All the nineteen compounds were evaluated for their ability to inhibit CVB3 in a classical antiviral assay. The study is designed to evaluate the dose dependent inhibition of cytopathic effect induced by CVB3 in cell culture. None was found to be effective except one, compound **17** (Table 1). Compound **17** inhibited CVB3 at a concentration of EC_{50} = 1.0 ±0.1 µM with a selectivity index of >140. Compound **17** was further evaluated against CVB4, poliovirus type1, enterovirus71 and rhinovirus14 (a small representative panel of viruses belonging to genus Enterovirus) to assess its spectrum/specificity. Interestingly it was found to inhibit only CVB4 from the representative panel at a concentration of EC_{50} = 16±3 µM, a concentration of 16-fold higher than it is required to inhibit CVB3. Thus, compound **17** was found to be specific towards CVB3. The carboxylic acid group at the fourth position of the phenyl ring in compound **17** seems to contribute towards its activity. Further simulation studies were performed to understand the reason for its specificity.

2.3 Molecular docking and dynamics

The antiviral data suggests that compound **17** interacts more specifically with 3C protease of CVB3 than with that of CVB4, which are very closely related proteases (65.8% similarity and 36.8% identity). Therfore, comparative molecular docking was performed to com-

Table 1. Antiviral activity against Coxsackie virus in Vero A cells

Code	R	R1	CC50	CVB3 EC50 (µM)	CVB4 EC50 (µM)
1	H	H	>199	>166	>199
2	Methyl	Methyl	>182	>152	>182
3	Ethyl	Ethyl	>168	>140	>168
4	Isopropyl	H	>174	>145	>174
5	-[(CH2)5]-		>162	>135	134 ± 19
6	-[(CH2)2-N(CH3)- (CH2)2]-		>156	>130	>156
7	Phenyl	H	>159	>132	>159
8	2-Hydroxy Phenyl	H	>152	>127	>152
9	3-Methoxy Phenyl	H	>147	>123	>147
10	4-Methoxy Phenyl	H	>147	>123	>147
11	3-Chloro Phenyl	H	>146	>121	>146
12	4-Chloro Phenyl	H	160 ± 10	>121	>160
13	2-Methyl phenyl	H	>153	>128	>153
14	3-Methyl phenyl	H	>153	>128	>153
15	4-Methyl phenyl	H	75 ± 21	>128	>75
16	4-Ethyl phenyl	H	>148	>123	>148
17	Phenyl-4-carboxylic acid	H	>142	1.0 ± 0.1a	16 ± 3
18	1-Napthyl	H	>140	>117	>140
19	Phenyl ethyl	H	>148	>123	>148

Data in µM. Mean ± SD of >2 dose-response curves from >2 independent experiments; [a]= upon microscopic inspection, at least at 1 concentration of compound, the infected, treated cells resembled the uninfected, untreated cell control condition.

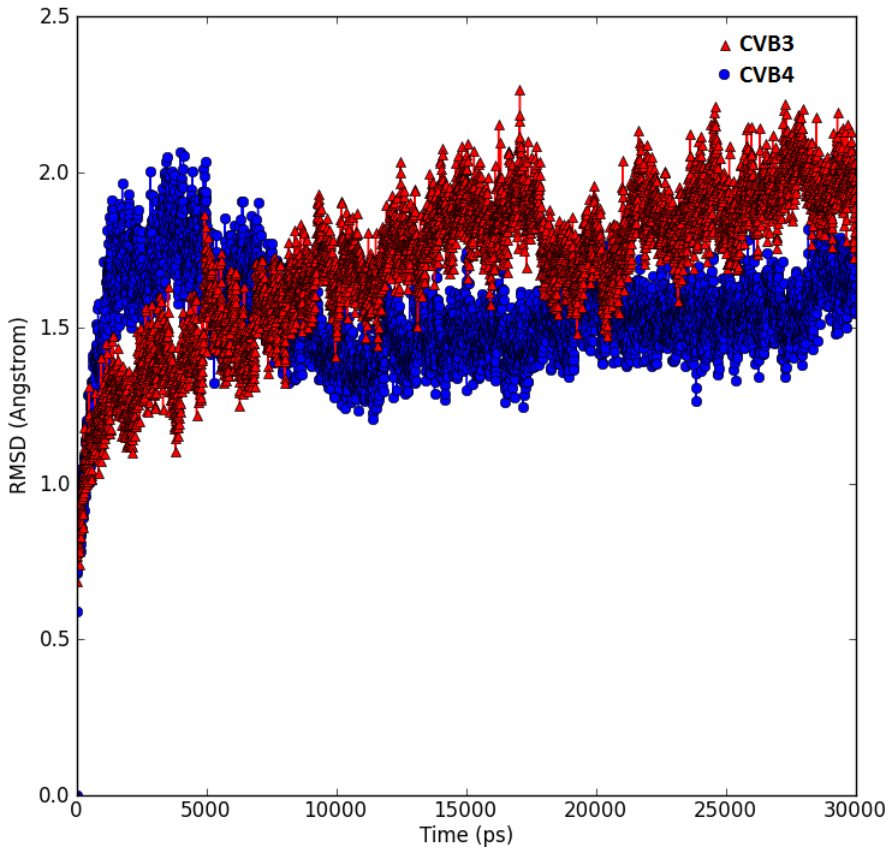

Figure 2. RMSD plot of the backbone MD simulation complex of compound **17** with the 3C protease of CVB3 and CVB4

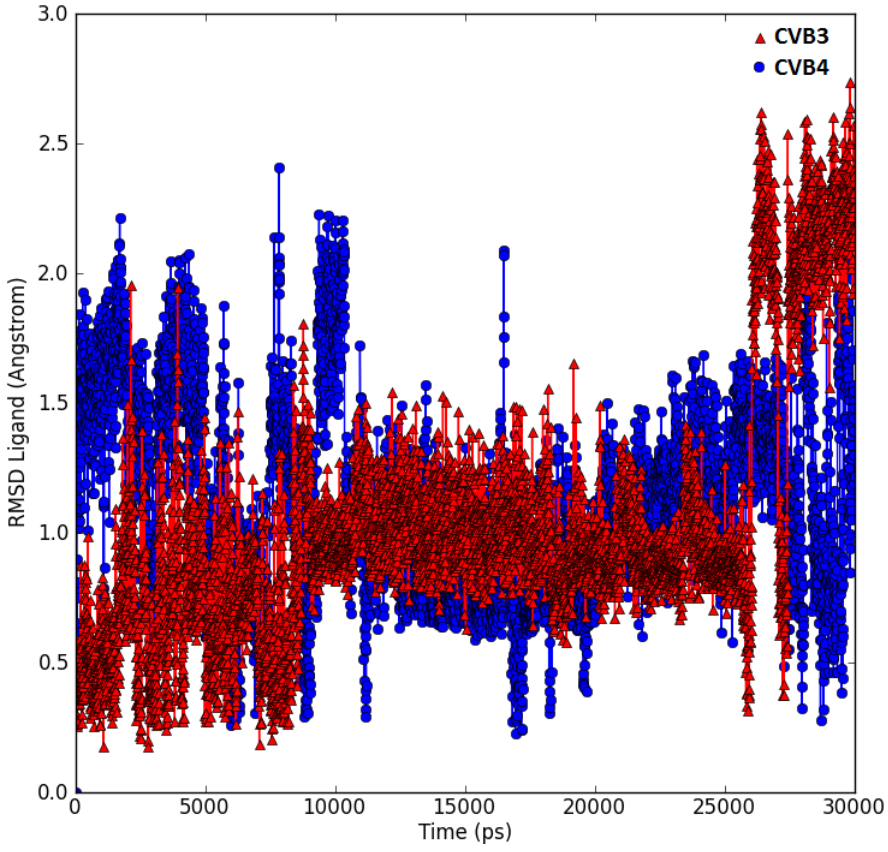

Figure 3. RMSD of compound **17** with the 3C protease of CVB3 and CVB4

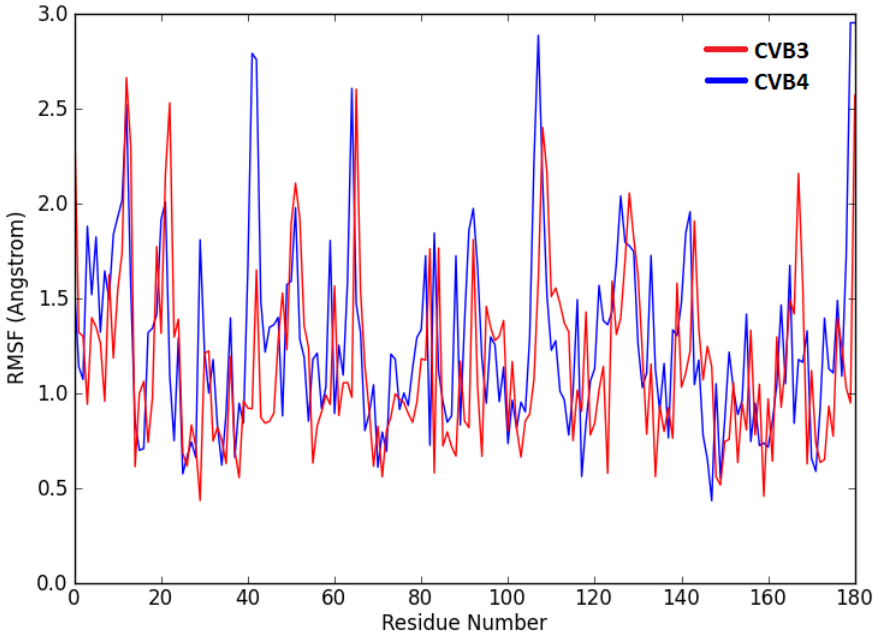

Figure 4. MD simulation trajectory analysis for RMSF of the backbone residues of the 3C protease of CVB3 and CVB4

pare the interaction of compound **17** with both the CVB3 and CVB4 3C proteases. The docked conformers were then subjected to MD simulation. We have studied RMSD (root mean square deviation), RMSF (root mean square fluctuation), radius of gyration (ROG), Intermolecular H-bond and energy were plotted as time-dependent function of MD simulations. RMSD of the protein backbone was found to be fluctuating around 1.1 to 2.2 Å and 1.3 to 2.0 Å for CVB3 and CVB4, respectively (Figure 2). Both proteins took different time intervals for converging. CVB4 converged immediately after 5ns while CVB3 took 20ns of simulated time. RMSD of compound **17** with 3C protease of CVB3 and CVB4 (Figure 3) suggests that, both the complexes are relatively stable. RMSF of all residues were calculated during 30 ns of simulated time to identify higher flexible regions of the protein (Figure 4). 3C protease residues of CVB3 were quite stable and were fluctuating less than 2.5 Å. This is comparable with the observations for CVB4, for which this is less than 2.8 Å, only slightly higher. But, the residues 40-45 of CVB4 are more flexible, where catalytic triad residue (His40) is present. This suggests that there is a possibility of these residues being more flexible may be responsible for the decrease in activity relative to CVB4. The radius of gyration (ROG) was analyzed to study protein compactness variation with simulated time. ROG of the CVB3-ligand complex ranges from 15.18 to 15.54 Å while that for the CVB4-ligand complex ranges from 15.16 to 15.52 Å, which suggests that protein/ligand complexes are stable without any noteworthy expansion/contraction in the overall protein/ligand complex (Figure 5). Plot of intermolecular H-bond between compound **17** and 3C proteases of CVB3 and CVB4 are given in Figure 6. This plot suggests that, the overall H-bonding between compound **17** and 3C protease of CVB3 is relatively higher than that of CVB4.

H-bond interaction with Val162, Gly164 and Asn165 play a major role for activity. Compound **17** has good H-bond interaction with the above mentioned residues for 3C protease of CVB3, whereas, for that of CVB4, although Gly164 is showing good H-bond, its interaction with remaining residues are poor, which may be one of the reason for specificity of Compound **17.** Finally, energy involved for stabilizing protein-ligand complex were observed to be -4998.9 KCal/mol for 3C protease of CVB3 and -4904.3 KCal/mol for that of CVB4 (Figure 7 and Table 2) which suggest that, ligand-protein complex of compound **17** with 3C protease of CVB3 is more stable than that of CVB4. These differences in the interaction of compound **17** with the 3C proteases of CVB3 and CVB4, may be resulting in a 16-fold difference in potency. Protein-ligand interactions were monitored and a histogram plot was presented in Figure 8 and the interactions were summarized Table 3. The average protein-ligand interaction during the simulation is given in Figure 9. The overall percentage of H-bond, ionic and hydrophobic interaction of compound **17** with 3C protease of CVB3 is better than that of CVB4, and the flexibility of residues near catalytic site of 3C protease of CVB4 may be responsible for specificity of compound **17** to CVB3 than CVB4. Table 4 summarizes the overall statistical analysis of MD simultion carried out.

3. Conclusion

As a result of this study, a novel antiviral compound with a benzene sulfonamide skeleton was obtained using *in silico* strategies based on the crystal structure of the 3C protease of Coxsackie virus B3. A series of nineteen novel benzene sulfonamide derivatives were synthesized and the evaluation of the antiviral activity in a virus-cell-based assay provided compound **17**, a potent and specific inhibitor of CVB3. MD simulation studies demonstrated that the difference in activity between CVB3 & CVB4 is mainly attributed to the difference in H-bond, ionic bond and hydrophobic interactions of compound **17** towards CVB3 and CVB4 along with flexibility near catalytic residue His40 of 3C protease of CVB3/CVB4. Before embarking in further biological studies to confirm that the 3C protease is the target of compound **17** & to further investigate its precise molecular mechanism of action, additional molecules will need to be synthesized in order to obtain inhibitors with antiviral activity in the sub-micromolar range, which will facilitate such studies.

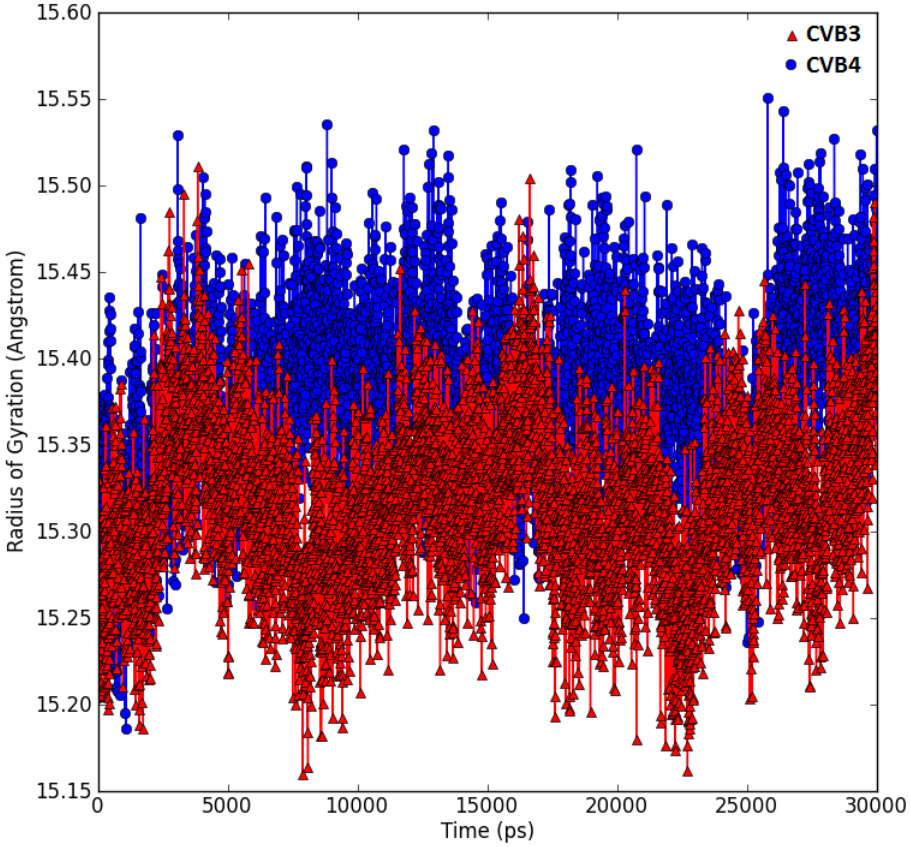

Figure 5. MD simulation trajectory analysis of the 3C protease-compound **17** complex for radius of gyration analysis of CVB3 and CVB4

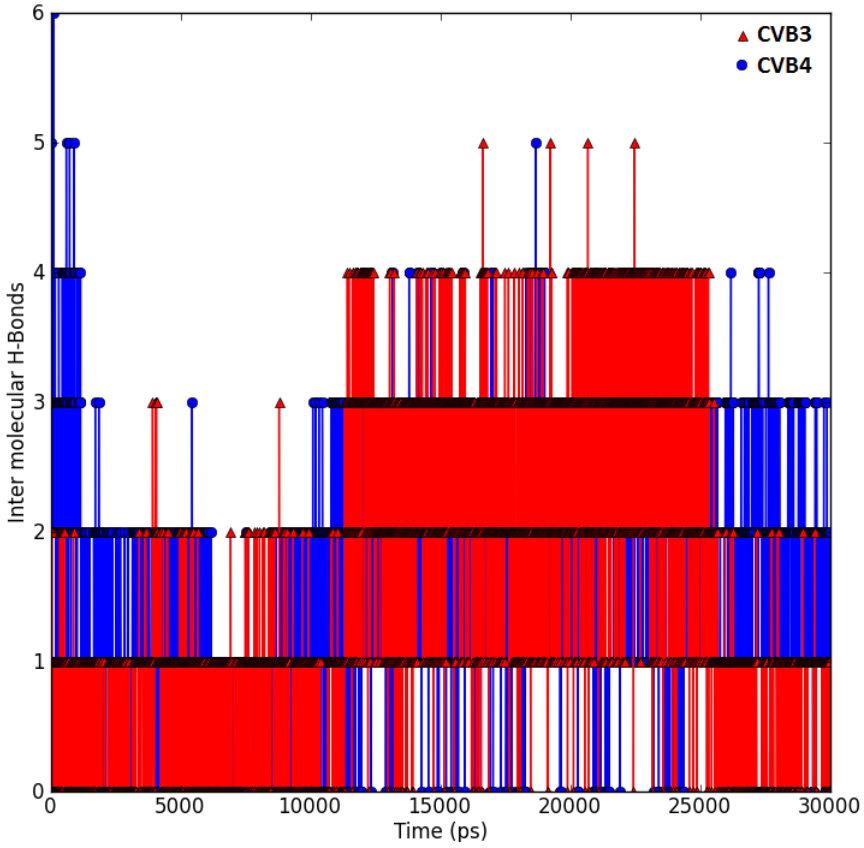

Figure 6. MD simulation trajectory analysis of compound **17** with 3C protease of CVB3 and CVB4 for intermolecular H-bonding

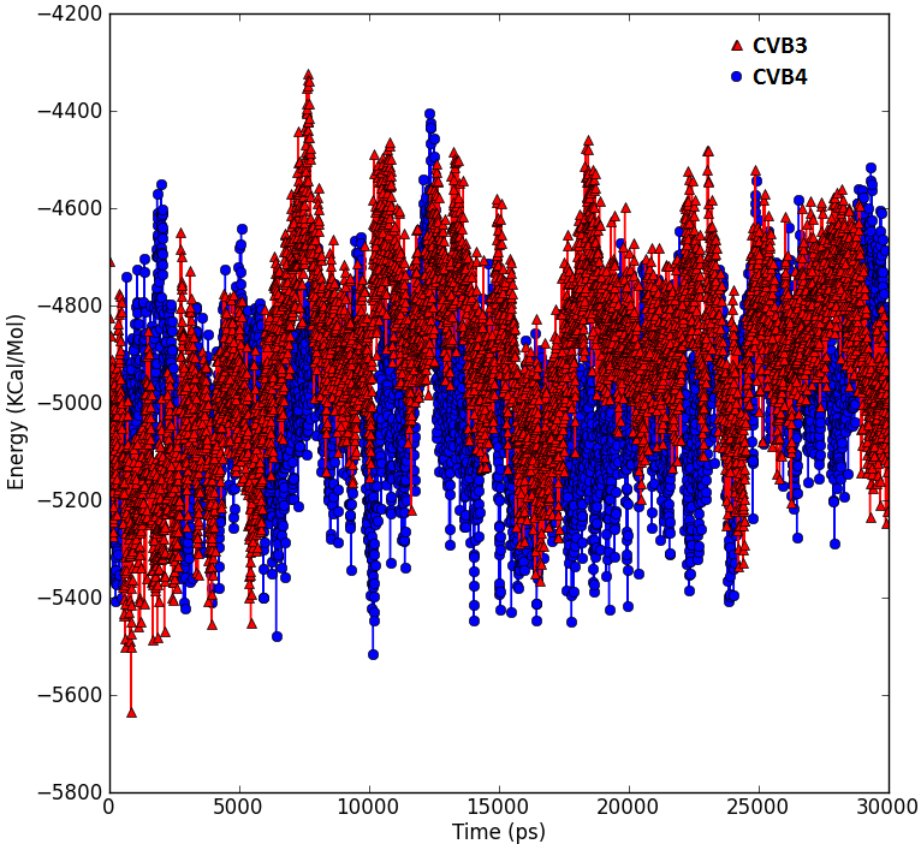

Figure 7. MD simulation trajectory analysis of compound **17** with 3C protease of CVB3 and CVB4 for energy

Furthermore, the synthesis of additional compounds will also allow to explore whether or not this series of compounds can be modified as such that compounds can be obtained with antiviral activity against a broader spectrum of enteroviruses.

Table 2. Comparative docking of compound **17** in the 3C protease of CVB3 and CVB4

3C protease	Glide XP Score	Contribution (Kcal/mol)		
		VdW	H-bond	ES
CVB3	-5.17	-2.51	-2.08	-0.8
CVB4	-3.03	-2.96	-0.67	-0.54

VdW-Van der Walls, ES-Electrostatic

4. Experimental

Materials and methods: Chemicals and solvents were of reagent grade and were purchased from Sigma-Aldrich/Merck/CDH/Rankem. Completion of reactions was monitored on TLC plates (Merck™ KGaA, Germany). Melting points were determined on an OPTIMELT (Stanford research systems, UK), an automated system apparatus and are uncorrected melting points. Final compounds were characterized by their ^{1}HNMR (400 MHz) in DMSO-d_6 solvent. ^{13}CNMR was recorded in Bruker AMX 300 NMR spectrometer with tetra methyl silane (TMS) as internal standard. In the ^{1}HNMR Spectra the coupling constants (J) are expressed in hertz (Hz). Chemical shifts (δ) of NMR are reported in parts per million (ppm) units relative to TMS. Mass spectra were recorded by WATERS-Q-T of Premier-HAB213 using the (ESI-MS) Electro-spray Ionization technique. Computational simulation studies were carried on DELL Workstation with Intel (R) Core (TM) i5-3330 Processor CPU @ 3.00 GHz and 8 GB DDR RAM. Schrodinger software was compiled and run under Linux CentOS 6.4 operating system. Docking and MD simulation snapshots were rendered using Schrodinger's Maestro interface v9.5.

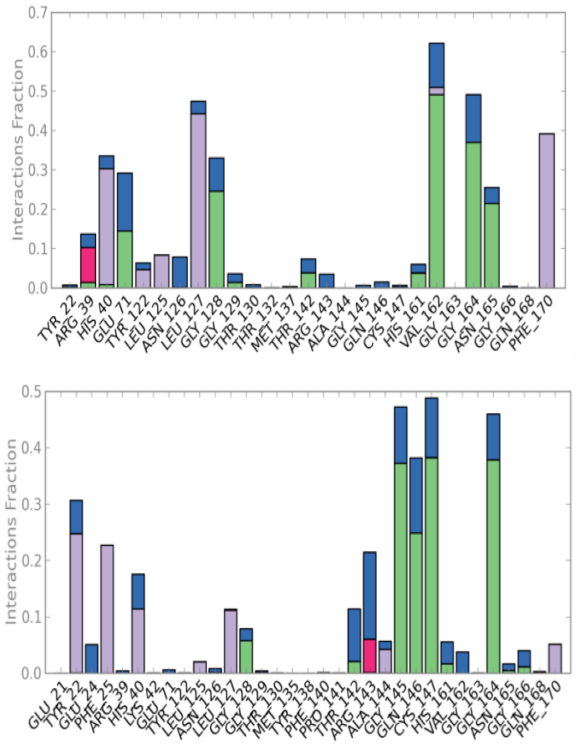

Figure 8. Analysis of the protein-ligand interactions that are involved in the stabilization of compound 17 within the 3C protease of CVB3 (top) and CVB4 (bottom). Violet: Hydrophobic : Blue: Water bridges Green: H-bonds ; Red: ionic

Table 3. Average interaction of compound **17** with CVB3 and CVB4 after MD simulation

Res	% Interaction for CVB3			
	H-bond	H_2O bridge	Hydrophobic	Ionic
Arg39	1.5	2.5	--	10
His40	--	4	29	--
Glu71	13	16	--	--
Tyr122	--	2	5	--
Leu125	--	--	9	--
Leu127	--	4	42	--
Gly128	22	9	--	--
Gly129	2	5	--	--
Thr142	5	3	--	--
Arg143	--	5	--	--
His161	5	2	--	--
Val162	50	10	2	--
Gly164	38	12	--	--
Asn165	21	5	--	--
Phe170	--	--	39	--
Res	**% Interaction for CVB4**			
	H-bond	**H_2O bridge**	**Hydrophobic**	**Ionic**
Tyr22	--	6	24	--
Phe25	--	--	23	--
His40	--	6	12	--
Leu127	--	--	12	--
Gly128	6	3	--	--
Thr142	2	9	--	--
Arg143	--	15	--	5
Ala144	--	2	4	--
Gly145	38	10	--	--
Gln146	25	11	--	--
Cys147	39	10	--	--
Gly164	39	7	--	--
Phe170	--	--	5	--

Table 4. Statistical analysis for the MD simulations trajectory of CVB3 and CVB4 protein ligand complexes

3C protease – Ligand complex	Energy (Kcal./mol)	
	Range	Mean
CVB3	[-5514.965, -4405.879]	-4998.869
CVB4	[-5634.321, -4323.584]	-4904.299

4.1 Chemistry

For the synthetic procedure and characterization data of the library compounds **(1-19)**, readers are suggested to refer our earlier publication[26].

4.2 Virus-cell-based assays

Coxsackievirus B3 strain Nancy and enterovirus 71 strain BRCR were obtained from F. Van Kuppeveld (University of Utrecht, The Netherlands), Coxsackievirus B4 strain E2 Edwards was received from J.W. Joon (University of Calgary, Canada), poliovirus 1 strain Sabin from A.J. Macadam (NIBSC, UK), and rhinovirus type 14 from K. Andries (J&J, Belgium). Vero A, RD (ECACC85111502), HeLa Rh or BGM cells were sub-cultured in cell growth medium [MEM Rega3 medium (Life Technologies, Cat. N° 19993013) with FCS (10%; Gibco), L-glutamine (5 mL, 200 mM; Gibco, 25030024) and $NaHCO_3$ (0.075%; Gibco, 25080060)]. They are prepared in tissue culture flasks (150 cm^2, Techno Plastic products) at a ratio of 1:10 (RD, HeLa Rh) or 1:4 (Vero A and BGM) and kept for 3-4 days or for 7 days before harvesting. The antiviral assays were performed in the same medium with only 2% FCS and in case of rhinovirus, medium with 30mM $MgCl_2$ was used. One day prior to assay setup, the cells were seeded in assay medium in 96-well microtiter plates (Falcon, BD) at a density of 25.000 cells/well in medium and allowed to adhere overnight in an incubator (37 of 25.000 cell-99% RH). The next day, a 2x compound dilution series was prepared in the medium present on top of the cells after which 100 µL medium (treated, uninfected controls) or 100 mL of a 2x virus inoculum (a virus dilution that was normalized to be as low as possible and still to induce a full cytopathic effect at the desired assay end point) was added. After setup, the assay plates were returned to the incubator for 3-4 days, a time at which maximal cytopathic effect is observed in the untreated, infected control conditions.

For the quantification of the antiviral and anti-metabolic effects, the assay medium was aspirated, followed by addition of 75 µL of a 5% MTS (Promega) solution in phenol red-free medium and incubation for 1.5 h (37 °C, 5% CO_2, 95-99% relative humidity) until an optical density (OD value) in the range of 0.6-0.8 was obtained. Absorbance was recorded at a wavelength of 498 nm (Safire^2, Tecan) and converted to percentage of untreated controls.

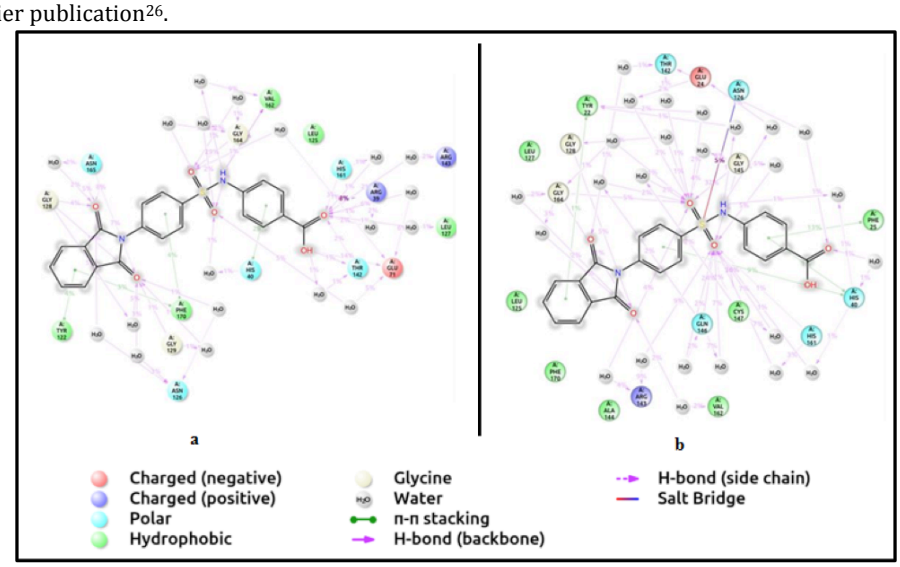

Figure 9. Schematic of the detailed atomic interactions of compound 17 with 3C protease residues of a) CVB3 and b) CVB4

Analysis of the raw data, quality control and calculation of the EC_{50} value was performed employing a custom-made data processing software package (Accelrys). The EC_{50} (value derived from the dose-response curve) represents the concentrations at which 50% inhibition of virus-induced cell death is observed. A compound is only considered as a selective inhibitor of virus replication when at least at one concentration, full inhibition of virus-induced cell death is observed without any apparent effect on host cell or monolayer morphology after microscopic inspection.

4.3 Molecular docking

The structure of the compound **17** was sketched using "build" tool while ZINC12 download from web (www.zinc-docking.org, drug-like subset filtered further using openeye FILTER tool) and prepared for docking using "Ligprep" utility (employing default parameters) in Maestro-9.3 (Schrodinger LLC). X-ray crystal structure of the CVB3 protease (PDB: 3ZZA[32]) was downloaded from the protein databank (http://www.rcsb.org/pdb). As crystal structure for CVB4 protease was not available, it is modeled through "Prime" module in Maestro-9.3 using the CVB4 protease sequence (UniprotKB AC: Q86887||15392-1720)[33] and the X-ray crystal structure of 3C protease of human Enterovirus 93 (PDB Code: 3Q3Y)[34] as they are having a sequence identity of 96%. Both the proteins were prepared for docking using "Protein preparation wizard" (employing default parameters) and grid was generated for docking using "Receptor grid generation" (grid box dimension 30Åx30Åx30Å centred over catalytic triad) module in Maestro-9.3.

Ligand docking was performed using Glide tool implemented in Maestro-9.3. For high-throughput virtual screening of ligands from ZINC12 database, HTVS protocol in Glide was employed. From the top 100 hits, different scaffolds are manually picked (Figure xx). A pthalimido-sulfonamide was chosen for enumeration of a small chemical library (Table 1). For compound **17**, XP protocol in Glide was employed. In both the cases default parameters were used for study.

4.4 Molecular dynamics

Docked conformer of compound **17** with 3C protease of CVB3 and CVB4 were used for further Molecular dynamic simulation with 'Desmond v3.6 Package'[35]. Predefined TIP3P water model[36] was used to simulate water molecules using OPLS2005 force field[37]. Orthorhombic periodic boundary conditions were set up to specify the shape and size of the repeating unit buffered at 10 Å distances. Boundary conditions box volume was initially calculated as 251853 $Å^3$ and 229072 $Å^3$ before and after minimization respectively. To neutralize the system electrically, three chloride ions were added to balance the charge of the system and were placed at random positions in the solvated system. After building the solvated system containing the protein in complex with the ligand, the system was minimized and relaxed using the default protocol integrated within Desmond module with OPLS 2005 force field parameters. Molecular dynamic simulations were carried out with the periodic boundary conditions in the NPT ensemble[38]. The temperature and pressure were kept at 300 K and 1.01325 atmospheric pressure using Nose–Hoover temperature coupling and isotropic scaling[39], the operation was followed by running the 30 ns NPT production simulation and saving the configurations thus obtained at 5 ps intervals.

Acknowledgement

We would like to acknowledge Caroline Collard, Nick Verstraeten and Charlotte Vanderheydt for their excellent assistance in the collection of the antiviral data. This work was supported by Department of Biotechnology (Govt. of India) for providing financial support through one of its INDO-GERMAN project (BT/IN/GERMAN/15/DV/2010).

References

1. Bowles, N.; Olsen, E.; Richardson, P.; Archard, L. Detection of Coxsackie-B-virus-specific RNA sequences in myocardial biopsy samples from patients with myocarditis and dilated cardiomyopathy. Lancet 1986, 327 (8490), 1120-1123.
2. Dalldorf, G. The Coxsackie Viruses*. Am J Public Health Nations Health 1950, 40 (12), 1508-1511.
3. Dalldorf, G.; Sickles, G. M. An unidentified, filtrable agent isolated from the feces of children with paralysis. Science 1948, 108 (2794), 61-62.
4. Javett, S.; Heymann, S.; Mundel, B.; Pepler, W.; Lurie, H.; Gear, J.; Measroch, V.; Kirsch, Z. Myocarditis in the newborn infant: A study of an outbreak associated with Coxsackie group B virus infection in a maternity home in Johannesburg. J Pediatr 1956, 48 (1), 1-22.
5. Brightman, V.; Scott, T. M.; Westphal, M.; Boggs, T. An outbreak of coxsackie B-5 virus infection in a newborn nursery. J Pediatr 1966, 69 (2), 179-192.
6. Sainani, G. S.; Krompotic, E.; Slodki, S. J. Adult heart disease due to the Coxsackie virus B infection. Medicine 1968, 47 (2), 133-147.
7. Smith, W. Coxsackie B myopericarditis in adults. Am Heart J 1970, 80 (1), 34-46.
8. Knipe, D.; Howley, P. M.; Griffin, D.; Lamb, R.; Martin, M.; Roizman, B. Field's Virology. 2001, Vol 1, 5th Ed. Lippincott Williams & Wilkins, Philadelphia (EUA)
9. Abzug, M. J. Prognosis for neonates with enterovirus hepatitis and coagulopathy. Pediatr Infect Dis J 2001, 20 (8), 758-763.
10. Kawashima, H.; Ryou, S.; Nishimata, S.; Ioi, H.; Kashiwagi, Y.; Iizumi, M.; Takami, T.; Sasamoto, M.; Takekuma, K.; Hoshika, A. Enteroviral hepatitis in children. Pediatr Int 2004, 46 (2), 130-134.
11. van der Schaar, H. M.; Leyssen, P.; Thibaut, H. J.; De Palma, A.; van der Linden, L.; Lanke, K. H.; Lacroix, C.; Verbeken, E.; Conrath, K.; MacLeod, A. M. A novel, broad-spectrum inhibitor of enterovirus replication that targets host cell factor phosphatidylinositol 4-kinase IIIβ. Antimicrob Agents Chemother 2013, 57 (10), 4971-4981.
12. Si, X.; McManus, B. M.; Zhang, J.; Yuan, J.; Cheung, C.; Esfandiarei, M.; Suarez, A.; Morgan, A.; Luo, H. Pyrrolidine dithiocarbamate reduces coxsackievirus B3 replication through inhibition of the ubiquitin-proteasome pathway. J Virol 2005, 79 (13), 8014-8023.

13. Harki, D. A.; Graci, J. D.; Galarraga, J. E.; Chain, W. J.; Cameron, C. E.; Peterson, B. R. Synthesis and antiviral activity of 5-substituted cytidine analogues: identification of a potent inhibitor of viral RNA-dependent RNA polymerases. J Med Chem 2006, 49 (21), 6166-6169.
14. Abdel-Mageed, W. M.; Bayoumi, S. A.; Chen, C.; Vavricka, C. J.; Li, L.; Malik, A.; Dai, H.; Song, F.; Wang, L.; Zhang, J. Benzophenone C-glucosides and gallotannins from mango tree stem bark with broad-spectrum anti-viral activity. Bioorg Med Chem 2014, 22 (7), 2236-2243.
15. Lee, S. M.; Kim, S. M.; Lee, Y. H.; Kim, W. J.; Park, J. K.; Park, Y. I.; Jang, W. J.; Shin, H.-D.; Synytsya, A. Macromolecules isolated from Phellinus pini fruiting body: chemical characterization and antiviral activity. Macromol Res 2010, 18 (6), 602-609.
16. Liu, Q.; Wang, Y.-F.; Chen, R.-J.; Zhang, M.-Y.; Wang, Y.-F.; Yang, C.-R.; Zhang, Y.-J. Anti-coxsackie virus B3 norsesquiterpenoids from the roots of Phyllanthus emblica. J Nat Prod 2009, 72 (5), 969-972.
17. Deng, Y.-P.; Liu, Y.-Y.; Liu, Z.; Li, J.; Zhao, L.-M.; Xiao, H.; Ding, X.-H.; Yang, Z.-Q. Antiviral activity of Folium isatidis derived extracts in vitro and in vivo. Am J Chin Med 2013, 41 (04), 957-969.
18. Binford, S.; Maldonado, F.; Brothers, M.; Weady, P.; Zalman, L.; Meador, J.; Matthews, D.; Patick, A. Conservation of amino acids in human rhinovirus 3C protease correlates with broad-spectrum antiviral activity of rupintrivir, a novel human rhinovirus 3C protease inhibitor. Antimicrob Agents Chemother 2005, 49 (2), 619-626.
19. Gorbalenya, A.; Svitkin, Y. V.; Kazachkov, Y. A.; Agol, V. Encephalomyocarditis virus-specific polypeptide p22 is involved in the processing of the viral precursor polypeptides. FEBS Lett 1979, 108 (1), 1-5.
20. Padalko, E. New strategies for the treatment of coxsackievirus-induced myocarditis. 2005, p. 333, Leuven University Press, Leuven, Belgium
21. Kuo, R.-L.; Kung, S.-H.; Hsu, Y.-Y.; Liu, W.-T. Infection with enterovirus 71 or expression of its 2A protease induces apoptotic cell death. J Gen Virol 2002, 83 (6), 1367-1376.
22. Weng, K.-F.; Li, M.-L.; Hung, C.-T.; Shih, S.-R. Enterovirus 71 3C protease cleaves a novel target CstF-64 and inhibits cellular polyadenylation. PLoS Pathog 2009, 5 (9), e1000593-e1000593.
23. Li, M.-L.; Hsu, T.-A.; Chen, T.-C.; Chang, S.-C.; Lee, J.-C.; Chen, C.-C.; Stollar, V.; Shih, S.-R. The 3C protease activity of enterovirus 71 induces human neural cell apoptosis. Virology 2002, 293 (2), 386-395.
24. Tong, L. Viral proteases. Chem Rev 2002, 102 (12), 4609-4626.
25. Badrinarayan, P.; Narahari Sastry, G. Virtual high throughput screening in new lead identification. Comb Chem High Throughput Screen 2011, 14 (10), 840-860.
26. Timiri, A. K.; Selvarasu, S.; Kesherwani, M.; Vijayan, V.; Sinha, B. N.; Devadasan, V.; Jayaprakash, V. Synthesis and molecular modelling studies of novel sulphonamide derivatives as dengue virus 2 protease inhibitors. Bioorg Chem 2015, 62, 74-82.
27. Tang, G.; Lin, X.; Qiu, Z.; Li, W.; Zhu, L.; Wang, L.; Li, S.; Li, H.; Lin, W.; Yang, M. Design and synthesis of benzenesulfonamide derivatives as potent anti-influenza hemagglutinin inhibitors. ACS Med Chem Lett 2011, 2 (8), 603-607.
28. Bano, S.; Javed, K.; Ahmad, S.; Rathish, I.; Singh, S.; Alam, M. Synthesis and biological evaluation of some new 2-pyrazolines bearing benzene sulfonamide moiety as potential anti-inflammatory and anti-cancer agents. Eur J Med Chem 2011, 46 (12), 5763-5768.
29. Bashir, R.; Ovais, S.; Yaseen, S.; Hamid, H.; Alam, M.; Samim, M.; Singh, S.; Javed, K. Synthesis of some new 1, 3, 5-trisubstituted pyrazolines bearing benzene sulfonamide as anticancer and anti-inflammatory agents. Bioorg Med Chem Lett 2011, 21 (14), 4301-4305.
30. Ghorab, M. M.; Ragab, F. A.; Hamed, M. M. Design, synthesis and anticancer evaluation of novel tetrahydroquinoline derivatives containing sulfonamide moiety. Eur J Med Chem 2009, 44 (10), 4211-4217.
31. Brzozowski, Z. 2-Mercapto-N-(azolyl) benzenesulphonamides III. Synthesis of some new 2-mercapto-N-(5-amino-1, 2, 4-triazol-3-yl) benzenesulphonamide derivatives with potential anti-HIV or anticancer activity. Acta Pol Pharm 1995, 53 (4), 269-276.
32. Wang, H.-M.; Liang, P.-H. Picornaviral 3C protease inhibitors and the dual 3C protease/coronaviral 3C-like protease inhibitors. Expert Opin Ther Pat 2010, 20 (1), 59-71.
33. Kang, Y.; Chatterjee, N. K.; Nodwell, M. J.; Yoon, J. W. Complete nucleotide sequence of a strain of coxsackie B4 virus of human origin that induces diabetes in mice and its comparison with nondiabetogenic coxsackie B4 JBV strain. J Med Virol 1994, 44 (4), 353-361.
34. Costenaro, L.; Kaczmarska, Z.; Arnan, C.; Janowski, R.; Coutard, B.; Solà, M.; Gorbalenya, A. E.; Norder, H.; Canard, B.; Coll, M. Structural basis for antiviral inhibition of the main protease, 3C, from human enterovirus 93. J Virol 2011, 85 (20), 10764-10773.
35. Shivakumar, D.; Williams, J.; Wu, Y.; Damm, W.; Shelley, J.; Sherman, W. Prediction of absolute solvation free energies using molecular dynamics free energy perturbation and the OPLS force field. J Chem Theory Comput 2010, 6 (5), 1509-1519.
36. Jorgensen, W. L.; Chandrasekhar, J.; Madura, J. D.; Impey, R. W.; Klein, M. L. Comparison of simple potential functions for simulating liquid water. J Chem Phys 1983, 79 (2), 926-935.
37. Price, D. J.; Brooks, C. L. Detailed considerations for a balanced and broadly applicable force field: A study of substituted benzenes modeled with OPLS‐AA. J Comput Chem 2005, 26 (14), 1529-1541.

38. Shinoda, W.; Mikami, M. Rigid - body dynamics in the isothermal - isobaric ensemble: A test on the accuracy and computational efficiency. J Comput Chem 2003, 24 (8), 920-930.
39. Nosé, S. A unified formulation of the constant temperature molecular dynamics methods. J Chem Phys 1984, 81 (1), 511-519.